Mausam, (1985), **36**, 4, 491-498

552.576.1:551.553.21:551.507.362.9

Cloud characteristics of monsoon depressions as viewed by meteorological satellites

A. CHOWDHURY, P. S. URANKAR and C. U. UPADHYE

Meteorological Office, Pune

(*Received 25 September 1982*)

सार — अवदाब केन्द्र की सतह स्थिति के आस-पास 10 अंश अक्षांश/देशान्तर क्षेत्र को 2.5 अंश के ग्रिड वर्गों में बांट कर पश्चिम/पश्चिम-उत्तर-पश्चिम की ओर बढ़ने वाले मानसून अवदाबों के उपग्रह मेघ चित्रों की जांच की गई है। इस लेख में अवदाबों के साथ जुड़े बृहत् मापी प्रवाह पैटर्न के संबंध में माध्य मेघाच्छन्नता की सममान रेखाओं, विचरण के गुणाकों तथा दीर्घ तथा निम्न मेघाच्छन्नता के वरीय क्षेत्रों पर विचार विमर्श किया गया है। उपग्रह से प्राप्त चित्रों में मेघ-प्रारूपों का विस्तृत वर्ग दिखाई दिया है। इन चित्रों की सहायता से मानसून अवदाबों के विभिन्न क्षेत्रों में दैनिक वर्षा का अनुमान लगाने का प्रयास किया गया है।

ABSTRACT. Satellite cloud pictures of west/westnorthwest moving monsoon depressions have been examined by dividing the area 10 degree latitude/longitude around the surface position of the depressions centre, into 2.5 degree grid squares. The isopleths of mean cloudiness, coefficient of variation and preferred zones of large and low cloudiness are discussed in relation to the large scale flow pattern associated with the depressions. Broad category of cloud patterns have been identified in the satellite pictures. An attempt has been made to estimate daily rainfall in different sectors of the monsoon depression from these pictures.

1. Introduction

Over past 20 years satellite technology is widely and routinely being used by meteorologists of over 75 countries of the globe. In tropics with sparse network of surface observatories, satellite information is extremely valuable for identification and tracking of storms by satellite imageries. In view of importance of cloud patterns in satellite meteorology, satellite photographs have been studied by a number of workers. For the Indian area, the first study in the direction was made by Koteswaram (1961) who from the satellite cloud patterns in a tropical cyclone in Arabian Sea found that during the earlier stages of development, cloud distribution was markedly assymetric. Among other studies of tropical storms and depressions in the Bay of Bengal and Arabian Sea areas mention can be made of Srinivasan (1968), Mukherjee and Misra (1968), Ramaswamy (1971), Srinivasan *et al.* (1971) etc.

The aim of the study is to present climatology of satellite-observed cloudiness around monsoon depression centre in India. Characteristic patterns of the *satellite cloudiness in the field of monsoon depression* would also be discussed. Finally, it is proposed to estimate rainfall from the satellite clouding by suitably weighing cloud types in regions affected by depressions.

2. Data used and method of analysis

In the present study APT visual pictures recorded at Poona were utilised. All those depressions which formed in late June, July and August, during 1977 to 1981 and moved in W/WNW direction were studied. In all 40 case histories were obtained and analysed.

In this analysis, 20 degree latitude/longitude domain about surface position of the depression centre was considered. The area was divided into 64 grids, each of 2.5 degree latitude/longitude. For each of the 2.5 degree 'square' for all depression days, the actual cloud coverage as seen by the satellite was utilised. The cloud pictures pertain to NOAA satellites for 1977, 1978 and 1981 which passed over Poona between 0630 & 1030 IST and TIROS system in 1979 and 1980 having passes between 1400 & 1700 hrs. In determining the cloudiness no distinction was made between high and low clouds. For each depression and grid, the cloud information was extracted and

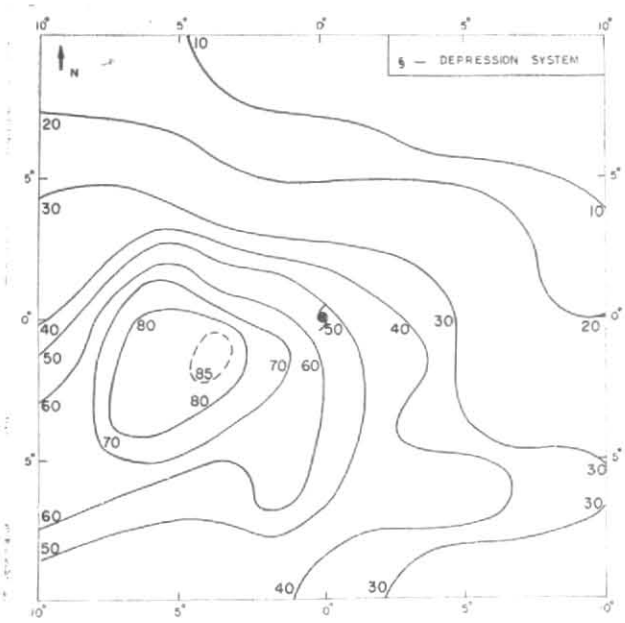

Fig. 1 (a). Mean satellite determined cloudiness (%) around monsoon depression centre
[*Read* : Dep. centre *instead* dep. system]

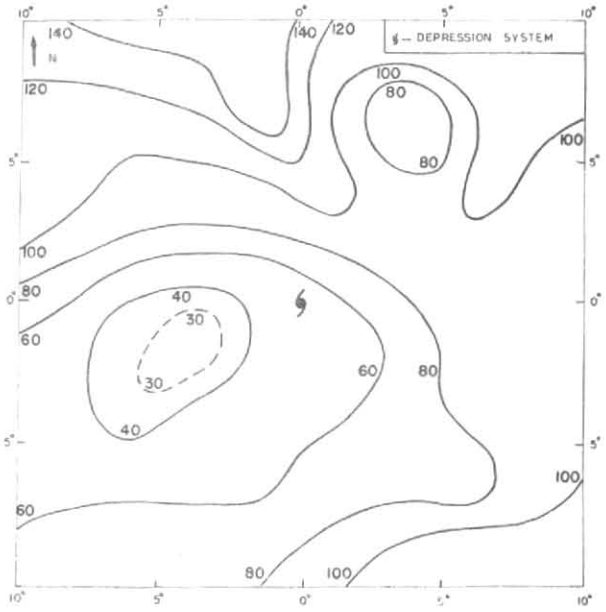

Fig. 1 (b). Coefficient of variation (%) of the satellite determined cloudiness
[*Read* : Dep. centre *instead* dep. system]

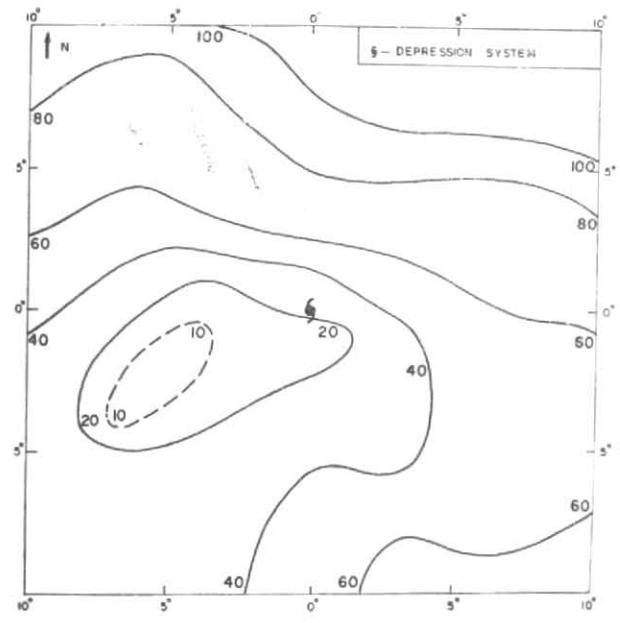

Fig. 2(a). Percentage frequency of days when 25 per cent or less of the area is covered with clouds
[*Read* : Dep. centre *instead* dep. system]

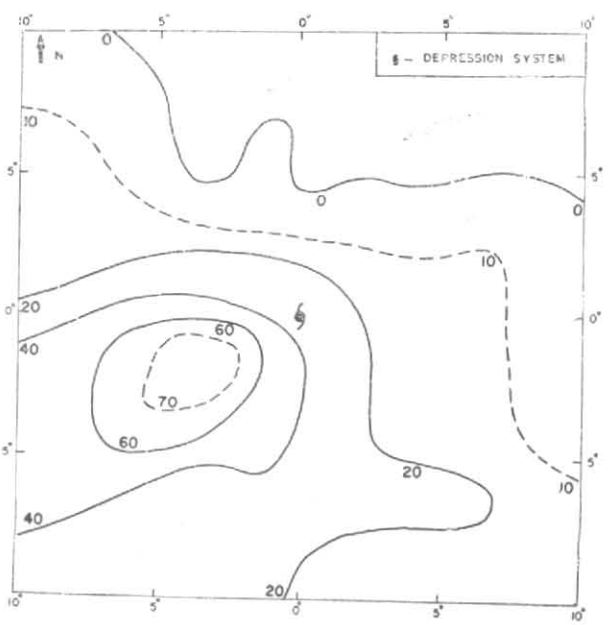

Fig. 2(b). Percentage frequency of days when 75 per cent or more of the area is covered with clouds
[*Read* : Dep. centre *instead* dep. system]

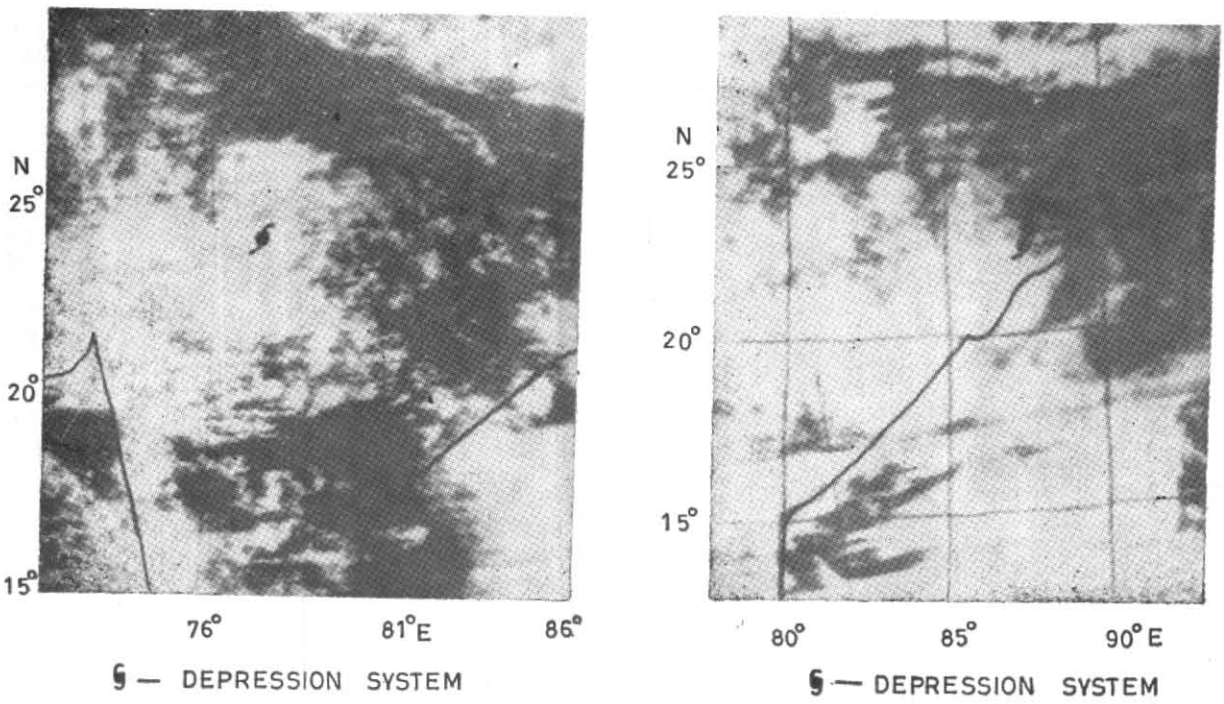

Figs. 3 (a&b). Satellite cloud photographs on (a) 30 August 1980 and (b) 14 August 1981

[*Read* : Dep. centre *instead* dep. system]

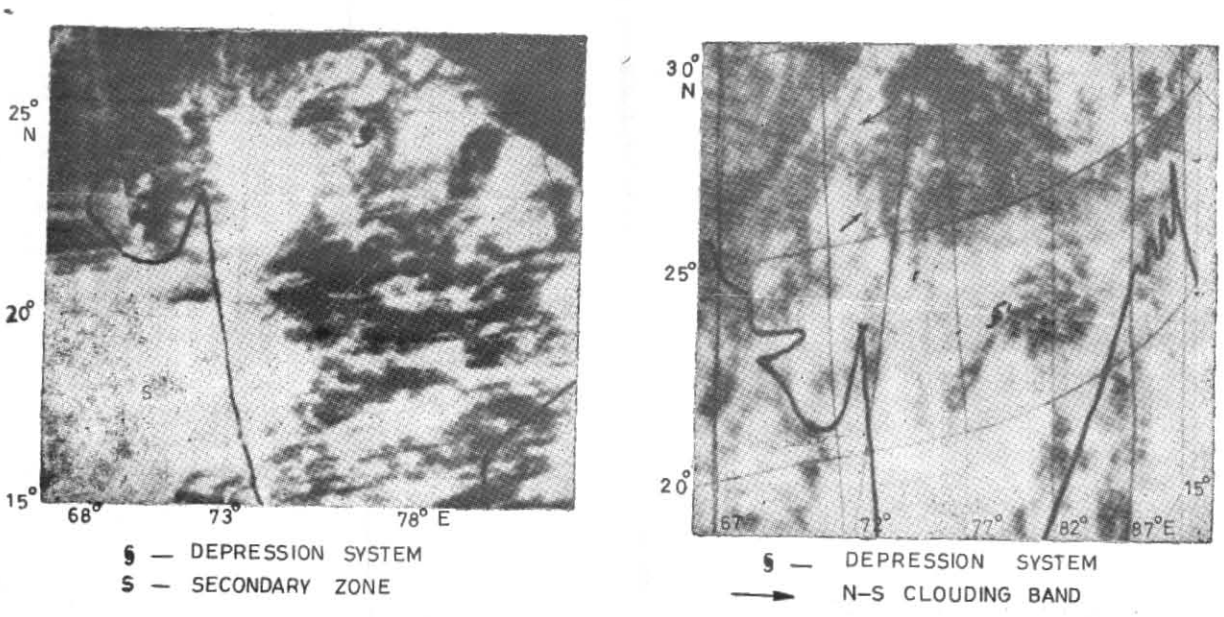

Figs. 3(c & d)

[*Read* : Dep. centre *instead* dep. system]

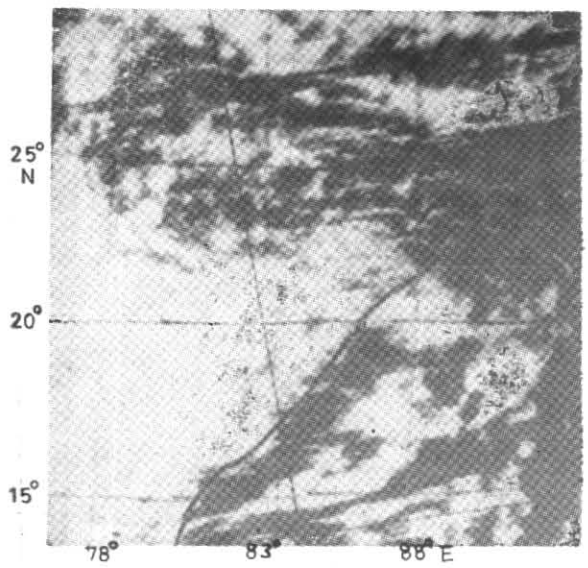

Fig. 3(e). Satellite cloud photograph on 15 Aug' 81. Centre of the depression was 50 km SW of Ambikapur (23.0° N, 83°. E)

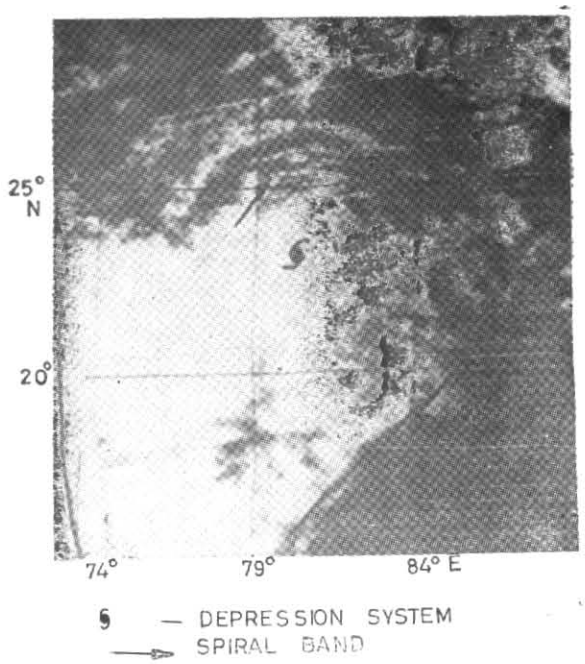

Fig. 3(f). Satellite cloud photograph on 9 Aug' 79

[*Read* : Dep. centre *instead* dep. system]

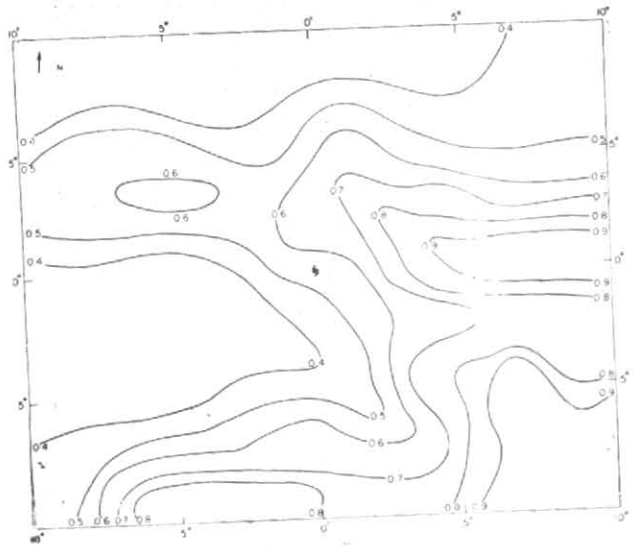

Fig. 4. Distribution of correlation field

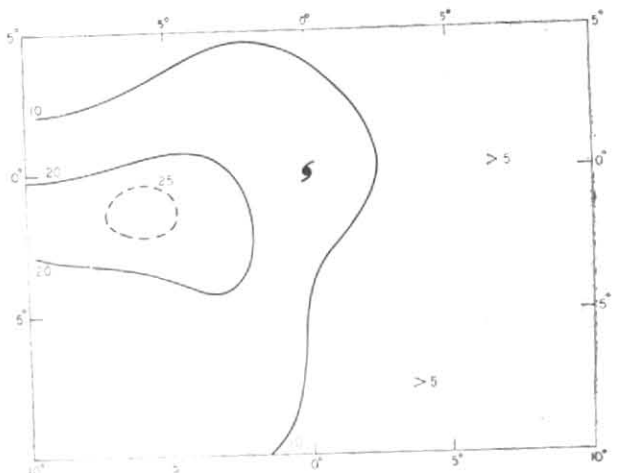

Fig. 5. Mean satellite derived daily rainfall (mm) around monsoon depression centre

averaged by the following method (*cf.* Sadler 1965).

Extent of cloud cover	*Range of cloudiness (%)*	*Assigned value*	*Approx. equivalent cloud amount (octas)*
Open or clear	0	0	0
Mostly open	Upto 25	1	1-2
Generally covered	25-50	3	3-4
Moderately covered	50-75	5	5-6
Heavily covered	75-100	7	7-8
Thickly covered	100	9	8

The assigned values were then averaged for each square mesh, converted into the mean cloudiness as per col. 2 above, plotted at the centre of each mesh and were subjectively analysed by drawing isopleths of mean cloudiness of different magnitude using linear interpolation. Areas with fewer than 10 observations in any square were not included in the analysis. The mean cloudiness in each of 2.5 degree grid squares was utilised to estimate areal rainfall.

3. Distribution of cloudiness

The mean cloudiness and its variations are discussed in the following paragraphs.

Fig. 1 (a) depicts the spatial distribution of mean cloud cover. The chief features of the satellite based pattern are as below :

(*i*) A belt of enhanced cloudiness exceeding 80 per cent is located 2 to 7 degrees southwest of the surface position of depression centre aligned generally in a southwest-northeast direction. Interestingly, this feature corresponds to the normally observed and preferred region of heavy rainfall associated with the low level convergence and upward motion taking place in the depression circulation field. Outwards of this zone, cloudiness decreases rapidly northward, particularly in the northwest. This greater gradient in cloudiness implies steeper moisture and rainfall gradients in this sector of monsoon depression. The decrease in the cloudiness elsewhere is rather smooth and gradual.

(*ii*) Clear skies (cloud cover less than 20 per cent) stretch from northwest of the depressions to its northeast. Another belt of supressed cloudiness is seen in the extreme southeast fringe of the field. The minimum in the north is pronounced and rather extensive and in the extremity of this extensive field merges with the low level easterly flow. It is well known that development of the cloud maxima and minima and gradient in cloudiness depend not only on moisture contents of the air and moisture gradient but also on the dynamical and physical processes which lift the moist air to produce cloudiness.

From the marked minimum observed in the north of the centre one would be tempted to infer that upward motion of air over this region is inhibited by subsidence. Presumably, this subsidence, is more effective in decreasing the cloudiness than the upward motion in increasing it.

The variation in the mean cloudiness was also examined by computing the coefficient of variation (CV). For each grid, the CV is plotted, analysed and depicted in Fig. 1(b).

It is seen that the areas of high CV are :

(*i*) northwest extreme, indicative of the passage of westerly systems like western disturbance,

(*ii*) Southeast corner suggesting occasionally large cloudiness perhaps in association with movement of easterly wave trough.

The area of lowest CV is about 3° southwest of the depression centre, where overcast conditions persist.

In order to bring out preferred areas of large and small cloudiness, occasions of occurrence of 25 per cent or less clouding and 75 per cent or more cloudiness were obtained, plotted and analysed in Fig. 2. The pattern is similar to that of the mean cloudiness (Fig. 1 a).

The analysis brings out the following features :

(*i*) Southwest of the depression centre, 25 per cent or less cloudiness occurs only in 10 to 20 per cent of occassions.

(*ii*) Almost clear skies prevail to north and northeast extremity of the depression field where the low level flow is easterly to northeasterly.

(*iii*) In 60 to 70 per cent of the occasions, the southwest sector is thickly clouded.

The observed zones of maximum and minimum cloudiness and the transition from one to the other are thus consistent with the current ideas about the mechanism of cloud development within monsoon depression field. A clear identification of mean cloud in the depression system and its definite association with the weather would perhaps not been possible but for the availability of satellite observations.

4. Cloud patterns

Examination of satellite pictures reveal that the cloud patterns associated with monsoon depression system are of large variety. The most common feature in all the pictures as pointed out by Srinivasan *et al.* (1971) is the presence of a distinct, vast and central dense overcast cloudiness (CDO) in the southwest of the surface position of the depression centre. This cloud mass is relatively brighter than the clouds present in the neighbourhood. Other features of the cloud mass and the cloud features found in this study are as below :

The CDO is normally amorphous, has a radius of 2.5 to 3.0 Lat./Long. (Fig. 3 a) and is generally composed of stratiform clouds though within the cloud layer, isolated cumuliform clouds are seen. An interesting feature observed is about the nature of cloudiness near the surface position of the depression centre. In nearly 50 per cent of the cases studied, the centre was within the dense layer of cloud mass. However, in the remaining half of the cases, not only the centre was

cloud-free but this cloud-free zone was sometimes rather extensive advancing into other sectors of the depression field (Fig. 3 b). This cloud free zone is more prominent in the north and northwest. The northward penetration was upto 2 to 3 degrees latitude but its southward extension was observed in very few cases and its projection limited to less than 1 degree. Nature of weather activity near the centre has been examined by Chowdhury (1983). He found that the weather near the centre is rather subdued, due perhaps to slow subsidence motion. It appears this subsidence zone under favourable circumstances is not confined to depression centre but sometimes extends in the north and northwest sectors.

Another feature found in the analysis is an occasional presence of a distinct cloud zone away from the CDO (Fig. 3 c), consisting mostly of cumuliform clouds. This secondary zone is situated southwest/west of the depression centre and is perhaps related to the secondary belt of heavy rainfall observed by Chowdhury and Gaikwad (1983).

A north-south band of cloudiness was also observed to join the general clouding in the northwest sector of the depression field (Fig. 3 d). This belt was seen in nearly a third of the cases analysed. In the mean, the zone has about 2 deg. longitude width and 5 deg. latitude as its northward extension and was located about 7 to 8 deg. from the centre. Examination of synoptic charts revealed that nearly in all such cases, the cloud belt could not be related to passage of western disturbance. It is, therefore, believed that the north-south oriented cloud system seen in the northwest sector is part of the depression system.

A feature of considerable importance seen in this study is an occasional presence of cloud free zone off Orissa-Andhra coasts. This is particularly seen when the depression is over land east of 80 deg. E and preferably over east Madhya Pradesh (*see* Fig. 3 e).

The sea water over this coastal strip is the warmest during monsoon (NAVAIR 1974). Thus, presence of cloud-free zone east of the depression centre when the system is over land is perhaps due to interaction of the cold monsoon current in the depression field with the comparatively warm sea water, the effect due to former dominating that of the latter, supressing the upward motion.

Banded structure of the clouds in the northwest sector of the depression centre is an accepted and prominent feature of the satellite clouding. However, though Srinivasan *et al.* (1971) found these bands in deepening stage of the depressions, no such association could be established in this study and these were observed irrespective of the stage of the depression. The number of bands also varied from one to as many as five in exceptional cases. They were observed 2 to 4 deg. northwest of the centre (Fig. 3 f) and though they normally terminated near east of the centre, sometimes they encompassed more than the semi-circle, terminating in the southeast sector of the depression.

5. Estimation of rainfall from satellite cloudiness

A number of rainfall estimation procedures are available which empirically relate satellite-viewed clouds to quantitative rainfall amounts. Lethbridge (1967) and Lethbridge and Panofsky (1969) have shown that rainfall probability increases,

(*i*) as temperature in the window radiation channel (8 to 12 μ) decreases and (*ii*) as cloud brightness increases.

Correlation between average satellite cloud cover and rainfall over S. Florida was obtained by Gerrish (1970).

Barrett (1970, 1971) utilised satellite nephanalysis to estimate monthly rainfall by evolving a rainfall coefficient. In developing the coefficient, he used mean monthly cloud cover probability of rainfall and its intensities from different cloud types.

In the studies cited above the rainfall is estimated by using the equation

$$R = (a_1c_1 + a_2c_2 + a_3c_3)/100$$

where R is the estimated rainfall (daily), a_1, a_2 and a_3 are empirical constants and c_1, c_2 and c_3 are respectively the percentage of cloud covered by cumulonimbus, stratiform and cumulus types of clouds respectively.

Follansbee (1973) assumed $a_1 = 1.0$, $a_2 = 0.25$ and $a_3 = 0.02$. Accordingly, the maximum rainfall that could be estimated would be 1 cm. The average rainfall received over extended areas, in monsoon being quite large, the coefficient a_1 was taken as 2.5, other coefficients remaining unaltered.

In this study morning/afternoon satellite pictures of the current day were used to estimate rainfall amounts recorded for 24 hr period ending 0830 IST of the next day. In the first instance, correlation (r) was obtained between the rainfall and the cloud cover (after weighing it according to the above coefficients), for each mesh of the field. In computing the correlations, meshes having less than 10 observation were not considered. The results are depicted in Fig. 4. Areas of correlation exceeding 0.9 occur beyond 5 deg. east of the depression centre and also over the southeastern end of the depression field. In another area SSW of the centre also the correlation between the cloud and rainfall is large. However, in the zone of heavy rainfall west/southwest of the centre the correlation is rather low (about 0.4).

The above technique has also been applied to different zones of the depression field. The results are given in Table 1. In each of the cases, the multiple correlation coefficient is found significant, though the correlations are somewhat large in the rear sectors of the depression compared to the forward sector.

Reliability of correlation coefficient has been determined by computing its probable error e from the following equation :

$$e = 0{\cdot}6745\ \frac{1 - r^2}{\sqrt{N}}$$

Where N is the number of observations and r is the correlation coefficient.

The probable error is also given in Table 1.

In general, a correlation coefficient six times as large as the probable error is considered a good indication of mathematically good relationship. The correlations, for different areas obtained in the study are found 15 to 40 times as large as the probable error and as such the correlations are not only significant but also reliable.

Contingency tables relating rainfall estimates for satellite cloud coverage according to the above technique with the actual raingauge observations, have also been prepared. this has been done for the entire depression field around the depression centre and the four sectors. The contingency tables for each of these cases are given in Table 2. The selected class intervals (in mm of rainfall) are 0 to 10, 10 to 20, 20 to 50, 50 to 100, 100 to 150 and 150 to 200. In more than two-third of the instances, the class interval of the

TABLE 1

Correlation coefficient (r) and its probable error (e)

Area	Coefficient (r)	Probable error (e)	Ratio (r/e)
20° square around depression centre	0.507	0.013	39.0
15° square	0.497	0.025	19.9
10° square	0.508	0.023	22.1
5° square	0.583	0.039	14.9
Right rear sector	0.724	0.023	31.5
Left rear sector	0.605	0.028	21.6
Right forward sector	0.540	0.024	22.5
Left forward sector	0.407	0.027	15.1

TABLE 2

Contingency table relating observed daily rainfall to estimated daily rainfall

Obs. interval	Estimated class interval							Difference in class interval		
	0-10	10-20	20-50	50-100	100-150	150-200	Totals	Obs. interval	Frequency	% frequency
(a) 20° square around the depression centre										
0-10	699	118	35	0	0	0	852	Zero	821	65
10-20	53	58	59	0	0	0	170	One	339	27
20-50	25	73	60	10	0	0	168	Two	88	7
50-100	6	27	26	4	0	0	63	Three	8	1
100-150	0	2	1	0	0	0	3	Four	0	0
150-200	1	0	0	0	0	0	1	Five	1	0
Total	784	278	181	14	0	0	1257			
(b) 15° square around the depression centre										
0-10	462	84	28	0	0	0	574	Zero	553	63
10-20	33	45	49	0	0	0	127	One	251	28
20-50	22	53	44	7	0	0	126	Two	72	8
50-100	6	21	25	2	0	0	54	Three	8	1
100-150	0	2	1	0	0	0	3			
150-200	0	0	0	0	0	0	0			
Total	523	205	147	9	0	0	884			

TABLE 2 (*contd.*)

Obs. interval	Estimated class intervals						Total	Difference in class interval		
	0-10	10-20	20-50	50-100	100-150	150-200		Obs. interval	Frequency	% frequency
(c) 10° square around the depression centre										
0-10	209	53	15	0	0	0	277	Zero	270	58
10-20	22	31	29	0	0	0	82	One	149	32
20-50	13	29	29	4	0	0	75	Two	40	9
50-100	2	12	12	1	0	0	27	Three	4	1
100-150	0	2	0	0	0	0	2			
150-200	0	0	0	0	0	0	0			
Total	246	127	85	5	0	0	463			
(d) 5° square around the depression centre										
0-10	45	19	2	0	0	0	66	Zero	71	57
10-20	9	14	6	0	0	0	29	One	46	37
20-50	4	10	12	0	0	0	26	Two	6	5
50-100	1	0	2	0	0	0	3	Three	1	1
100-150	0	0	0	0	0	0	0			
150-200	0	0	0	0	0	0	0			
Total	59	43	22	0	0	0	124			
(e) Right rear sector										
0-10	155	12	0	0	0	0	167	Zero	176	88
10-20	6	21	0	0	0	0	27	One	23	11
20-50	1	5	0	0	0	0	6	Two	2	1
50-100	0	1	0	0	0	0	1			
100-150	0	0	0	0	0	0	0			
150-200	0	0	0	0	0	0	0			
Total	162	39	0	0	0	0	201			

TABLE 2 (*contd.*)

Obs. interval	Estimated class interval						Total	Difference in class interval		
	0-10	10-20	20-50	50-100	100-150	150-200		Obs. interval	Frequency	% frequency
(f) Left rear sector										
0-10	179	6	3	0	0	0	188	Zero	192	83
10-20	12	8	5	0	0	0	25	One	31	13
20-50	4	7	5	0	0	0	16	Two	8	4
50-100	0	1	1	0	0	0	2			
100-150	0	0	0	0	0	0	0			
150-200	0	0	0	0	0	0	0			
Total	195	22	14	0	0	0	231			
(g) Right forward sector										
0-10	221	3	19	0	0	0	243	Zero	270	68
10-20	22	5	32	0	0	0	59	One	87	22
20-50	12	16	43	5	0	0	76	Two	36	9
50-100	3	5	9	1	0	0	18	Three	4	1
100-150	0	1	0	0	0	0	1			
150-200	0	0	0	0	0	0	0			
Total	258	30	103	6	0	0	397			
(h) Left forward sector										
0-10	152	1	101	0	0	0	254	Zero	206	48
10-20	16	2	41	0	0	0	59	One	104	25
20-50	9	7	49	5	0	0	70	Two	114	26
50-100	3	2	34	3	0	0	42	Three	3	0.7
100-150	0	0	2	0	0	0	2	Four	0	0.0
150-200	1	0	0	0	0	0	1	Five	1	0.3
Total	181	12	227	8	0	0	428			

estimated rainfall is found to be the same as the class intervals of the observed rainfall. In the left forward sector such cases, however, were comparatively less, *viz.*, 50 per cent. When the class intervals coincide, the estimates are considered perfect. About 10 to 25 per cent of the class differed by just one class interval, which amounted to more than 90 per cent of the cumulative frequency, except again in the left forward sector where it is nearly 75 per cent. Thus, most of the rainfall estimates fall either in the correct category or one interval removed therefrom. Hardly in one or two instances, the estimates differed by more than two class intervals and these cases relate to stations affected by abrupt heavy to very heavy falls.

In the above rainfall estimation, cloud cover over a region during the pass of the satellite is assumed to represent the cloud cover for the entire day. This is an inherent limitation in the study since the cloud cover is likely to undergo diurnal variations.

6. Mean satellite-derived rainfall

From the correlations computed between the rainfall and the clouds in different grids, it is possible to estimate the rainfall. An attempt has been made in this paper to estimate mean satellite observed rainfall for 20 deg. square around the monsoon depression centre from the equation given in section 5. The results are depicted in Fig. 5. Though there appears to be a slight under estimation of rainfall, in the southwest sector, the general pattern however corresponds to what has been observed by Chowdhury and Gaikwad (1983). As such, even in the satellite derived rainfall the maxima is located in the southwest sector slightly away from the centre. In other sectors, the rainfall amounts, more or less, are similar to that observed. Thus it is felt the satellite information can be easily utilised for forecasting of rainfall, on a day to day basis, in the monsoon season when the depressions are forming and moving across the country to a reasonable degree of accuracy.

Most of the earlier approaches to widespread precipitation mapping have been based on comparative observations of cloud and hydrometer observations by ship and land based stations (*see* for example, Tucker 1961). The difficulties with which they are fraught were so great that comparable assessment of precipitation mapped by different workers have shown only small measure of agreement with each other. Relatively small number of poor agreements in this investigation cannot minimise the importance of the technique proposed for estimating the general structure of broad scale precipitation field.

7. Conclusions

The following results emerge from the study :

(*i*) A zone of maximum cloudiness is located 3 to 4 degrees southwest of the depression centre which could be identified as the principal area of heavy rainfall.

(*ii*) North and southeast extremity of the depression field is an area of suppressed cloudiness.

(*iii*) Five broad satellite cloud patterns could be identified in association with monsoon depression.

(*iv*) Cloud cover bears significant correlation with the rainfall in different regions of the depression field.

Acknowledgement

The authors are grateful to Shri H. M. Chaudhury, Additional Director General of Meteorology (Research) Pune and Shri A. K. Banerjee, Meteorologist, for their keen interest in the work and useful suggestions. Thanks are also due to Shri B. H. Godbole for preparing the computer programme and to Shri P. T. Vaz for typing the text.

References

Barrett, E.C., 1970, The estimation of monthly rainfall from satellite data, *Mon. Weath. Rev.*, **28**, pp. 322-327.

Barrett, E.C., 1971, The Tropical Far East : ESSA satellite evolution of the high season climatic pattern, *The Geocgr J.* **137**, pp. 535-555.

Chowdhury, A., 1983, Distribution of equivalent potential temperature in the field of monsoon depressions, *Mausam*, **34**, pp. 213-218.

Chowdhury, A. and Gaikwad, S. D, 1983, Some characteristic features of rainfall associated with monsoon depressions over India, *Mausam*, **34**, pp. 33-42.

Follansbee, W.A., 1973, Estimation of average daily rainfall from satellite cloud photographs, NOAA Tech. Memo. NESS 44.

Gerrish, H. P., 1970, Satellite and Radar analysis of mesoscale features in the tropics. Final Report. ECOM-0205 S-F, U.S. Army Electronic Command, 45 pp.

Koteswaram, P., 1961, Cloud patterns in a tropical cyclone in the Arabian Sea viewed by TIROS 1 Met. Satellite, Hawai, Inst. Geophys. Rep. 18, p. 34.

Lethbirdge, M., 1967, Precipitation probability and satellite radiation data, *Mon. Weath. Rev.*, **95**, pp. 487-490.

Lethbridge, M. and Panofsky, H. A., 1959, Satellite radiation measurement and synoptic data. Final Report Grant No. WBG-48, Pennsylvania State Univ., 35 pp.

Mukherjee, A. K. and Misra, P. K., 1968, Satellite study of a Bay cyclone, *Indian J. Met. Geophys.*, **19**, pp. 295-304.

NAVAIR, 1976, *Marine Climatic Atlas of the World*, 3, Indian Ocean Naval Weather Service Detachment, Asheville.

Ramaswamy, C., 1971, Satellite determined cloudiness in the tropics in relation to large scale flow patterns, Part I : Studies of different phased of the Indian southwest monsoon, *Indian J. Met. Geophys.*, **22**, pp. 289-294.

Sadler, J.C., 1965, Satellite meteorology in the International Indian Ocean Expedition. Proc. Symp. Met. results of IIOE Bombay, pp. 269-284.

Srinivasan, V., Raman, S. and Ramakrishnan, A. R., 1971, Monsoon depressions as seen in Satellite pictures, *Indian J. Met. Geophys.*, **22**, pp. 337-339.

Srinivasan, V., 1968, Some aspects of broad scale cloud distribution over Indian Ocean during Indian southwest monsoon season, *Indian J. Met. Geophys.*, **19**, pp. 39-45.

Tucker, G. B., 1961, Precipitation over North Atlantic Ocean, *Quart. J. R. Met. Soc.*, **94**, pp. 127-130.

Woodley, W. L., Sancho, B. and Miller, A. H., 1972, Rainfall estimation from Satellite cloud photographs : NOAA Tech. Memo. ERL-OD-11, pp. 43.